Electronic Supplementary Material (ESI) for Nanoscale.

Substrate-free Graphene Oxide-based Micromotor for Rapid Adsorption of Antibiotic

Yue Dong, Chen Yi, Shanshan Yang, Jie Wang, Peng Chen, Xin Liu, Wei Du, Song Wang and Bi-Feng Liu

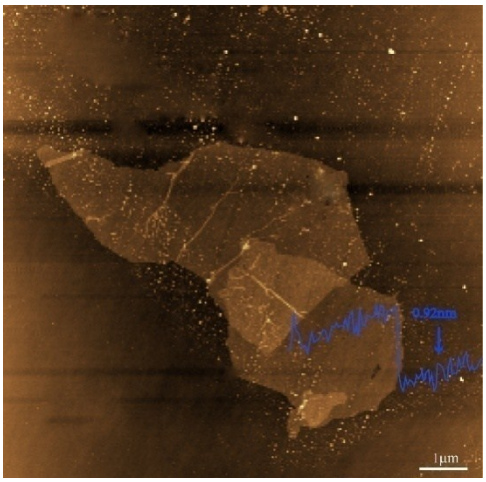

Figure S1. The AFM image of GO

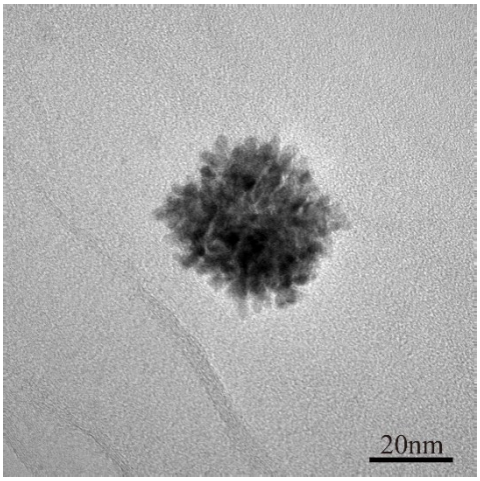

Figure S2. The enlarged TEM of Pt-GO, the hierarchical structure of Pt flower. The lattice of GO was clearly shown.

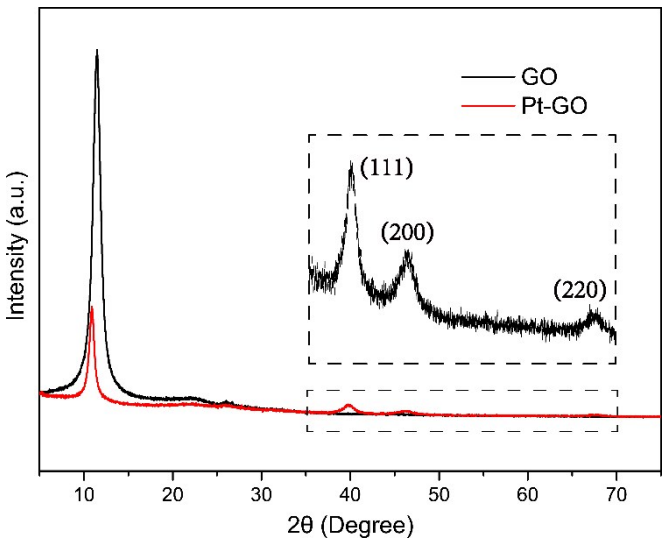

Figure S3. The XRD results of GO and Pt-GO (the inset is enlarged XRD result of Pt-GO)

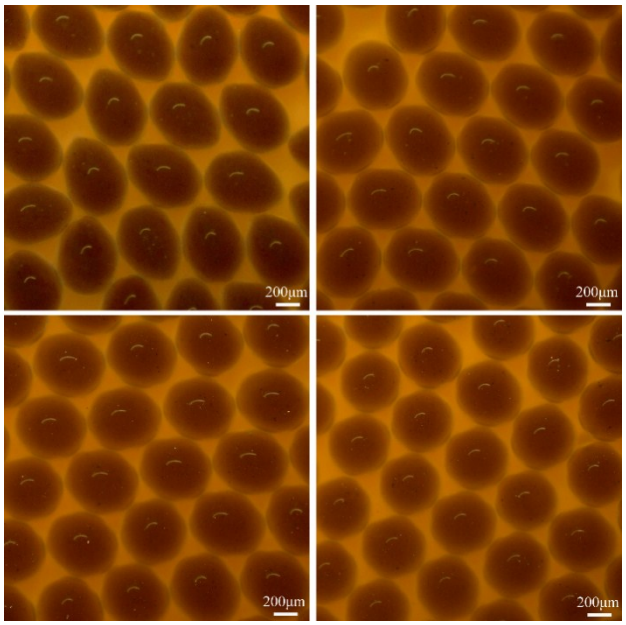

Figure S4. The droplets with different shape fabricated at the different concentration of GO and Pt-GO ranging from 10-20mg mL^{-1}

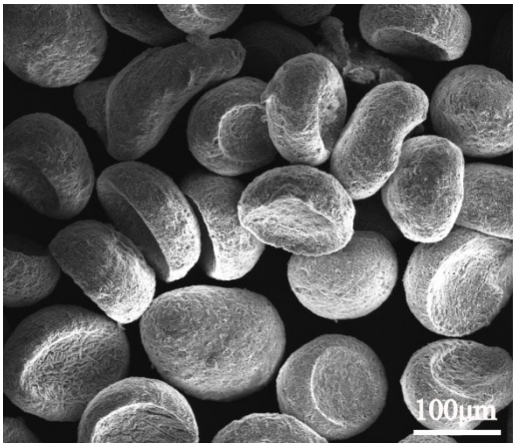

Figure S5. The micromotors with severe deformation fabricated at the concentration of (GO: 6mg mL^{-1}, Pt-GO: 6mg mL^{-1})

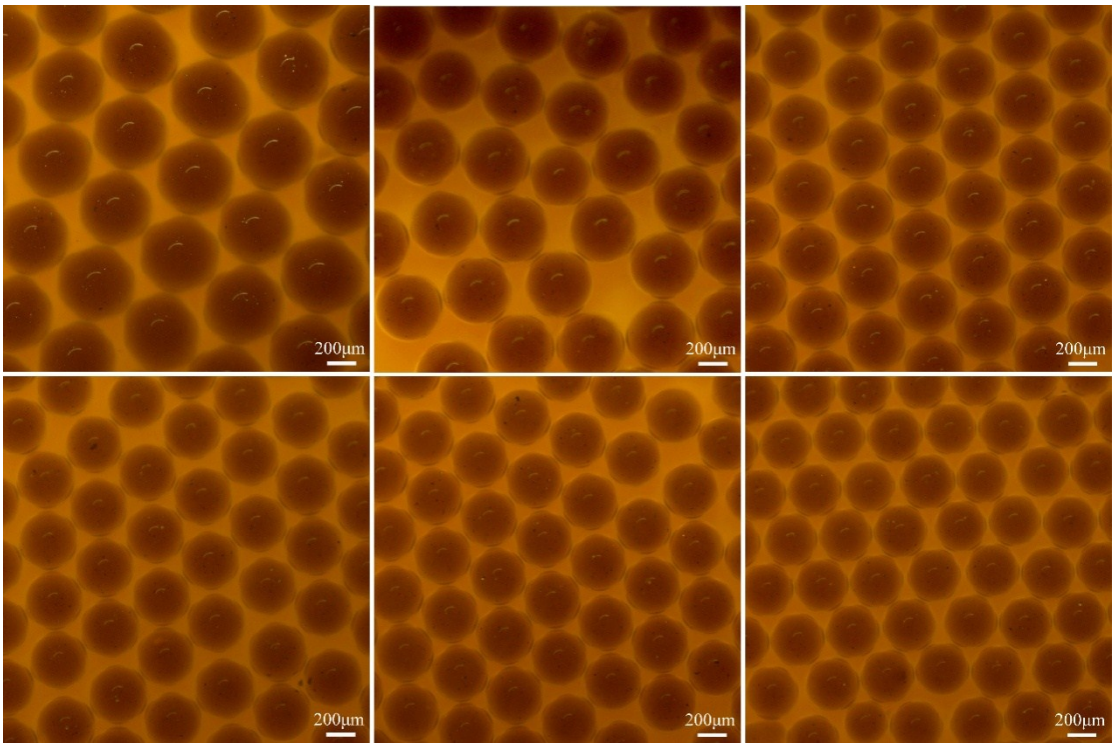

Figure S6. The droplets with different sizes fabricated at the different flow rates of oil phase ranging from 60 to 500 μl min^{-1}

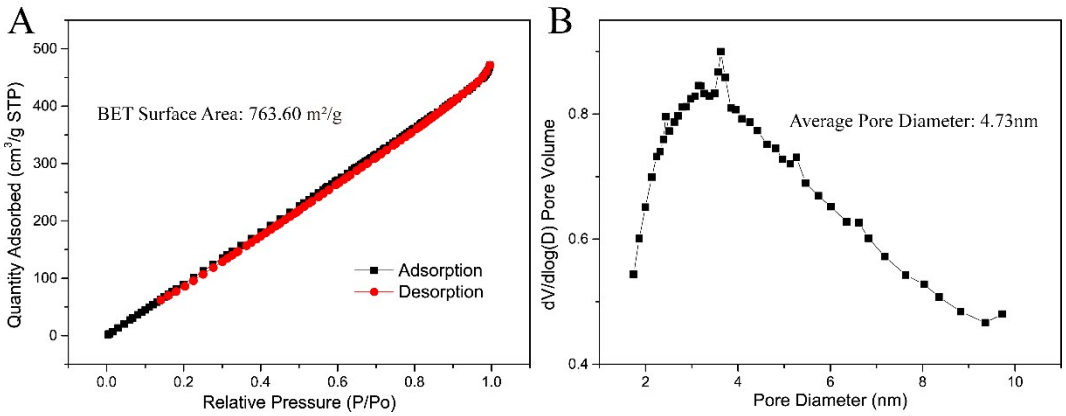

Figure S7. (A) Isotherm linear plot of micromotor, (B) The distribution of pore diameter for micromotors.

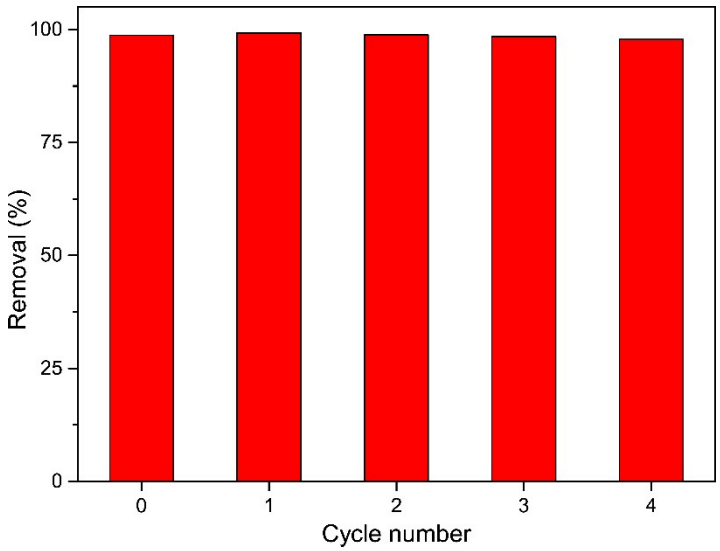

Figure S8. The reusability tests of the micromotors for tetracycline removal

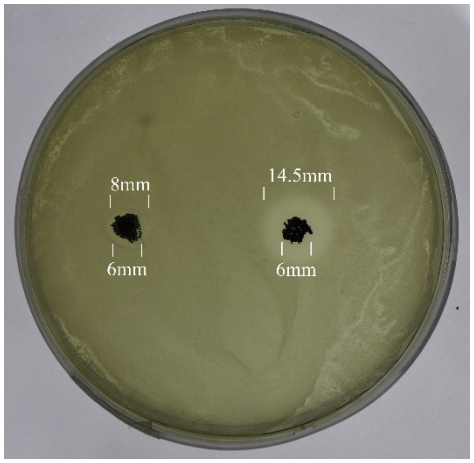

Figure S9. Zone of inhibition produced by micromotor with tetracycline adsorption and without tetracycline adsorption

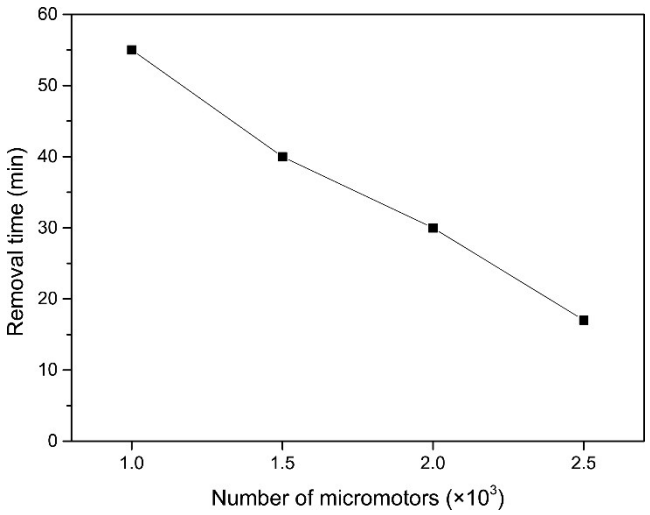

Figure S10. The effect of micromotor number on the removal time of tetracycline

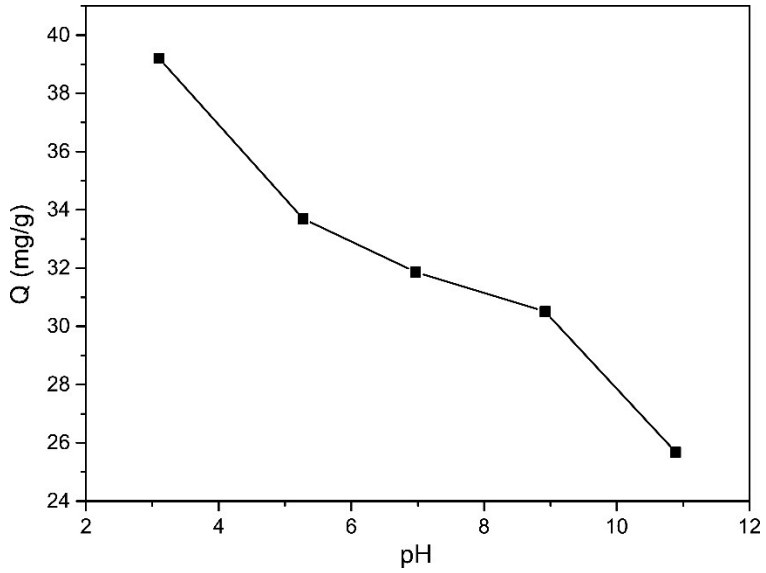

Figure S11. The effect of pH on the adsorption ability of micromotor

Table S1

Tetracycline		**First-order kinetic model**			**Second-order kinetic model**		
Co(mg mL^{-1})	q_e,exp (mg g^{-1})	k_1(g mg^{-1} min^{-1})	q_e,cal (mg g^{-1})	R^2	k_2(g mg^{-1} min^{-1})	*qe,cal (mg g^{-1})*	R^2
10	9.8 ± 0.5	0.146	12.5	0.913	0.0122	11.7	0.998
20	19.1 ± 0.7	0.113	16.6	0.934	0.0102	21.3	0.994
30	28.6 ± 1.4	0.153	29.8	0.924	0.0083	30.9	0.996